



# Identification, expression, and functional analysis of *Hsf* and *Hsp20* gene families in *Brachypodium distachyon* under heat stress

Na Li<sup>1,2,\*</sup>, Min Jiang<sup>1,3,\*</sup>, Peng Li<sup>1</sup> and Xiwen Li<sup>1,2</sup>

<sup>1</sup>Shanghai Key Laboratory of Plant Functional Genomics and Resources, Shanghai Chenshan Botanical Garden, Shanghai, China

<sup>2</sup>College of Life Sciences, Shanghai Normal University, Shanghai, China

<sup>3</sup>Ministry of Education Key Laboratory for Biodiversity Science and Ecological Engineering, Institute of Eco-Chongming (IEC), School of Life Sciences, Fudan University, Shanghai, China

\*These authors contributed equally to this work.

## ABSTRACT

**Background.** The heat shock factor (Hsf) and small heat shock protein (sHsp, also called Hsp20) complex has been identified as a primary component in the protection of plant cells from ubiquitous stresses, particularly heat stress. Our study aimed to characterize and analyze the *Hsf* and *Hsp* genes in *Brachypodium distachyon*, an annual temperate grass and model plant in cereal and grass studies.

**Results.** We identified 24 *Hsf* and 18 *Hsp20* genes in *B. distachyon* and explored their evolution in gene organization, sequence features, chromosomal localization, and gene duplication. Our phylogenetic analysis showed that BdHsfs could be divided into three categories and BdHsp20s into ten subfamilies. Further analysis showed that the 3'UTR length of *BdHsp20* genes had a negative relationship with their expression under heat stress. Expression analyses indicated that *BdHsp20s* and *BdHsfs* were strongly and rapidly induced by high-temperature treatment. Additionally, we constructed a complex regulatory network based on their expression patterns under heat stress. Morphological analysis suggested that the overexpression of five *BdHsp20* genes enhanced the seed germination rate and decreased cell death under high temperatures.

**Conclusion.** Ultimately, our study provided important evolutionary and functional characterizations for future research on the regulatory mechanisms of *BdHsp20s* and *BdHsfs* in herbaceous plants under environmental stress.

**Subjects** Bioinformatics, Genetics, Genomics, Molecular Biology, Plant Science

**Keywords** Heat shock protein, Heat shock factor, Evolution, Seed germination, *Brachypodium distachyon*, Correlation analysis

## BACKGROUND

Although plants may appear inactive, they have actually evolved a series of countermeasures to respond to various extracellular stimuli. Therefore, plants are not completely passive under external stresses and will form some complex protective mechanisms for adaptation. Abiotic stress, such as high temperature, high salt, heavy metal pollution, and drought, threaten crops' normal growth and development (Wang, Vinocur & Altman, 2003;

Submitted 26 April 2021  
Accepted 16 September 2021  
Published 1 October 2021

Corresponding author  
Min Jiang, yijinsha@126.com

Academic editor  
Mahmood-ur-Rahman Ansari

Additional Information and  
Declarations can be found on  
page 18

DOI 10.7717/peerj.12267

© Copyright  
2021 Li et al.

Distributed under  
Creative Commons CC-BY 4.0

OPEN ACCESS

*Mittler, 2006*). Global warming resulting from the greenhouse effect has made high temperatures a greater threat to plants and the main factor affecting plant productivity. It is well-known that heat shock factors (Hsfs) (*Nover et al., 2001*) and heat shock proteins (Hsps) (*Lindquist & Craig, 1988*) are initial response genes that can be rapidly induced to respond to high temperatures. Under external stimuli, *Hsp* expression can be induced by *Hsfs* binding the heat shock elements (HSEs; nGAAnnTTCn or nTTCnnGAAn) that exist in multiple copies upstream of the *Hsp* genes (*Giorno et al., 2010*). *Hsp* acts as a molecular chaperone that prevents protein misfolding and eliminates non-natural protein aggregation.

Hsps are widespread in living organisms and generally fall into five groups according to their molecular weight: Hsp100, Hsp90, Hsp70, Hsp60, and Hsp20 (*Marrs et al., 1993*; *Schirmer, Lindquist & Vierling, 1994*; *Krishna et al., 1995*; *Mayer & Bukau, 2005*; *Waters, 2013*). Hsp20 is a structurally conserved small heat shock protein (sHsp) with a molecular weight of 15–42 KD. It consists of a variable N-terminal region, a conserved C-terminal region, and a C-terminal extension region (*Kriehuber et al., 2010*; *Poulain, Gelly & Flatters, 2010*; *Waters, 2013*). The N-terminal region sequences across different subfamilies vary greatly, while their sequences in the same subfamily show high similarity (*Bondino, Valle & Have, 2012*). In contrast, the C-terminal sequence contains a conserved  $\alpha$ -crystallin domain (ACD), composed of approximately 90 amino acids, and can be divided into CRI and CRII regions with a  $\beta_6$ -loop junction in the middle region. sHsps are the “first responders” in response to cellular stress. They are ATP-independent chaperones that do not change the protein activity themselves, but instead bind to denature-modified proteins of the same molecular weight to form stable compounds and prevent their aggregation (*Hartl, Bracher & Hayer-Hartl, 2011*). For example, LimHSP16.45 and OsHSP18.2 are molecular chaperones that enhance cell viability under stress (*Mu et al., 2011*; *Kaur et al., 2015*). Additionally, abiotic stresses other than high temperature, such as drought, low temperature, high salt, heavy metals, anaerobic stress, and UV-light, can also induce sHsp synthesis (*Wang et al., 2004*; *Sun & Macrae, 2005*).

Unlike Hsps, Hsfs usually contain five conserved domains: the DNA binding domain (DBD), hydrophobic oligomerization domain (HR-A/B), nuclear localization signal domain (NLS), nuclear export signal (NES), and C-terminal activation domain (CTAD), which is characterized by short peptide motifs (AHA motifs). Hsfs can be divided into three subfamilies based on the number of amino acid residues inserted between HR-A/B: Class A, B, and C (*Guo et al., 2008*). Twenty-one amino acids were inserted in Class A, seven amino acids in Class C, and no amino acid residues in Class B (*Kotak et al., 2007*; *Scharf et al., 2012*). Hsf plays a key role in regulating plant responses to heat shock (*Lin et al., 2011*; *Ohama et al., 2016*), drought, salt, light, and cold stress (*Hwang et al., 2014*; *Zeng et al., 2016*; *Wang et al., 2020*) by regulating the expression of different *Hsps*. For example, three HSFs induced by heat stress were initially cloned and identified in tomato (*Solanum lycopersicum*) (*Scharf et al., 1990*). Although the role of Hsps and Hsfs in stress responses is well established, the regulatory network involved in stress tolerance and the many functions of Hsps need to be further studied.

*Brachypodium distachyon* ( $2n = 10$ ) is an annual temperate grass that has been widely accepted as a model plant. Its genome is completely sequenced in order to study characteristics that are unique to cereals and grasses (*International Brachypodium*, 2010; *Catalan et al.*, 2014). These characteristics include small stature, rapid life cycle, genetic tractability, self-fertility, and small diploid genome size (*Garvin et al.*, 2008; *Opanowicz et al.*, 2008). To obtain more detailed information, we performed correlation network and functional analysis of its Hsfs and sHsps. First, we identified and surveyed phylogenetic relationships of Hsfs and sHsps. Then, we investigated their evolutionary relationship in terms of 3D structure, chromosomal localization, gene duplication, and cis-elements. Next, the expression patterns of *Hsfs* and *sHsps* in different tissues and several abiotic stresses were evaluated, and we established the signaling regulatory network based on the expression patterns following different stress treatments. Finally, we measured the seed germination rate and trypan blue staining of five overexpressed BdsHsps in *Arabidopsis thaliana* after heat treatment.

## MATERIALS AND METHODS

### Sequence retrieval

The 23 Hsp20s and 21 Hsfs in *A. thaliana* (*Scharf, Siddique & Vierling*, 2001; *Sarkar, Kim & Grover*, 2009) and the 19 Hsp20s and 25 Hsfs in *Oryza sativa* (*Guo et al.*, 2008; *Sarkar, Kim & Grover*, 2009) were obtained from the Arabidopsis Information Resources database (TAIR: <http://www.arabidopsis.org/>) (*Lamesch et al.*, 2012) and the TIGR Rice Genome Annotation Resources database (<http://rice.plantbiology.msu.edu/>) (*Ouyang et al.*, 2007), respectively. These sequences were used to search for the Hsp20s and Hsfs in *B. distachyon* in the publicly available PLAZA database (<http://bioinformatics.psb.ugent.be/plaza/>) (*Bel et al.*, 2018). Collected sequences were scanned using InterPro software and were only considered if they possessed Hsp20 or Hsf consensus sequences, as confirmed by a previous study (*Mitchell et al.*, 2019). Any redundant or alternative splice variants were eliminated. Ultimately, we collected 18 Hsp20s and 24 Hsfs belonging to *B. distachyon*. Additionally, the molecular weights (Mw) and isoelectric points (pI) of Hsps and Hsfs were obtained from the ExPASy's pI/Mw calculation tool ([https://web.expasy.org/compute\\_pi/](https://web.expasy.org/compute_pi/)). Subcellular localization predictions for each protein were performed using the CELLO server (<http://cello.life.nctu.edu.tw/>).

### Gene structure, multiple sequence alignment, protein motif, and 3D structure analyses

The exon/intron organization of candidate Hsp20s and Hsfs were surveyed using Gene Structure Display Server (GSDS) software (<http://gsds.gao-lab.org/>; *Hu et al.*, 2015). The sequence alignments were carried out using Clustal Omega with default parameters (<http://www.ebi.ac.uk/Tools/msa/clustalo/>). The Hsp20 and Hsf domains and motifs were identified using MEME (<http://meme-suite.org/tools/meme>; *Bailey et al.*, 2015). Visualization of the protein-conserved domain of these genes was drawn using the WebLogo3 application (<http://weblogo.threeplusone.com/>). The 3D structure of the BdHsp20s and BdHsfs was modeled using PHYRE2 with default parameters (highest

percent identity, most sequence coverage) (<http://www.sbg.bio.ic.ac.uk/phyre2/html/page.cgi?id=index>).

### **Chromosomal locations, duplication, synteny, and phylogenetic analyses of *BdHsp20s* and *BdHsf*s**

We collected the chromosome location information of *BdHsp20* and *BdHsf* genes from the PLAZA database and visualized them using the CoreDRAW X3 program. Synteny information of duplicate genes was based on the PlantDGD database (<http://pdgd.njau.edu.cn:8080/>; Qiao *et al.*, 2019). Phylogenetic trees based on the alignment of *Hsp20* and *Hsf* full-length nucleotide or amino acid sequences were constructed using the maximum likelihood (ML) method with the Jones-Taylor-Thornton (JTT) model, 1000 bootstrap values, and partial deletion in MEGA 5.0 software for *O. sativa*, *A. thaliana*, and *B. distachyon*, respectively (Tamura *et al.*, 2011).

### **Cis-element analyses of *BdHsp20s* genes**

The upstream 2 kb sequences of the identified *BdHsp20* genes were downloaded from the PLAZE database. The extracted sequences were submitted to the PlantCARE website (<http://bioinformatics.psb.ugent.be/webtools/plantcare/html/>; Lescot *et al.*, 2002) for cis-elements analysis. The diagram of the cis-elements of *BdHsp20* genes was displayed using CorelDraw software.

### **Plant growth, treatment, and expression analysis**

Bd21 seeds were sown in 1/2 Murashige and Skoog (MS) medium in the dark for 4 d at 25 °C, transferred to a soil mix, and grown in a greenhouse with a cycle of 21 °C for 14 h of light and (>3000 lux)/18 °C for 10 h of darkness. Root, shoot, leaf, and caryopsis were collected from 2-week-old seedlings for tissue-specific expression analysis. For heat analysis, 2-week-old *B. distachyon* Bd21 plants were treated in liquid MS medium under 40 °C for 1 h, 3 h, 6 h, 12 h, and 24 h. For dark and UV analysis, 2-week-old *B. distachyon* Bd21 plants were treated in MS liquid medium for 1 h, 3 h, 6 h, 12 h, and 24 h. For abscisic acid (ABA) analysis, 2-week-old *B. distachyon* Bd21 plants were treated in MS liquid medium containing 100 μM ABA for 1 h, 3 h, 6 h, 12 h, and 24 h. Plants were harvested at their corresponding time points after treatment for further analyses. All samples were flash-frozen in liquid nitrogen and used for RNA extraction.

We extracted the total RNA from each sample using Trizol reagent, and reverse-transcribed 1–2 μg into cDNA using PrimeScript RT Master Mix Perfect Real-Time (TaKaRa, Kyoto, Japan) according to the manufacturer's instructions. The total RNA was detected for quality using Nanodrop1000 and its integrity was calculated by electrophoresis in 1.5% (w/v) agarose gel. The real-time quantitative polymerase chain reaction (RT-qPCR) was executed in 10 μl reactions with 5–50 ng of first-stand cDNA products (4 μl), 5 pmol of each primer (0.4 μl), 5 μl SYBR green master mix (2X), and 0.2 μl ROX as a passive reference standard to normalize the SYBR fluorescent signal. The RT-qPCR thermal profile was as follows: initial activation at 95 °C for 5 min followed by 45 cycles of 95 °C for 30 s and 60 °C for 30 s. Afterward, PCR product specificity was monitored using a melting curve analysis (61–95 °C with fluorescence read every 0.5 °C). The *B. distachyon actin* (*Bradi2g24070*)

gene was used as an internal reference for all RT-qPCR analyses. Each experiment was implemented with three independent biological replicates. The relative *BdHsp* and *BdHsf* gene expression was calculated using the  $2^{-\Delta\Delta C_t}$  method. The up-regulated genes were defined as a fold-change greater than 2 with a  $p$  value of  $< 0.05$ , and the down-regulated genes were less than 0.5 with a  $p$  value of  $< 0.05$ . The primer-sets are listed in [Table S1](#).

### **Regulatory network and pattern analyses of *BdHsp20* and *BdHsf* genes**

The length of the mRNA untranslated region (5'UTR and 3'UTR) can significantly affect mRNA stability and protein translation efficiency ([Srivastava et al., 2018](#)). To assess the relationship of 3'UTR length and the expression levels of the *BdHsp20* gene under heat stress, its correlation coefficient was investigated and the results were displayed in a linear graph. Additionally, the *BdHsp20* and *BdHsf* expression data were detected using RT-qPCR under heat stress and were clustered together to form an integrated expression profile. *BdHsf* and *BdHsp20* genes with correlation coefficients greater than 0.7 or less than  $-0.7$  were screened as a set of their expression regulatory, which we submitted into Cytoscape software ([Shannon et al., 2003](#)) to construct their correlation regulatory network.

### **Binary vector construction, Arabidopsis transformation, heat stress treatment, and trypan blue staining of the transgenic plants**

We amplified full-length cDNAs encoding *BdHsp20s* (including BdHsp16.9-CI, BdHsp17.2A-CI, BdHsp17.2B-CI, BdHsp18-CII, and BdHsp16.4-CI; [Table S2](#)) using a pair of specific primers ([Table S3](#)) from Bd21 plants, cloned them into pCambia1300 vector at BamHI/KpnI sites, and yielded corresponding plasmid 35S:BdHsp20s that were used for *Agrobacterium*-mediated Arabidopsis transformation. Positive transgenic plants were screened and planted on 1/2 MS medium containing 25  $\mu\text{g/L}$  hygromycin for one week. The presence of the transgenic insertion was confirmed by PCR in the transgenic plants. Homozygous T3 transgenic plants were subjected to 50 °C for 1 h during the seed germination experiment. More than 100 independent plant seeds were picked for the experiment, and Arabidopsis wild-type (WT) seed was used as the control. Each treatment was conducted in triplicate independently using three biological replicates. After two weeks, the morphological observation was recorded, and the germination rate was counted.

Dead cells were determined by trypan blue staining ([Cui et al., 2018](#); [Luan et al., 2018](#)) using the homozygous T3 transgenic plants. The T3 generation transgenic and WT seeds were treated at 50 °C for 1 h and then placed in normal growth conditions. The trypan blue staining solution contained LPTB: 25% w/v lactic acid, 2.5 mg/ml trypan blue, 25% glycerin, and 23% phenol water. The seedlings were placed in a vacuum machine and extracted for 10 min until the dye was completely injected into the plants. Afterwards, we added an appropriate amount of Chloral hydrate solution to the hood to repeat decolorization. After complete decolorization, equilibration for 2 h using 70% glycerol, and observation and photographing with a microscope, the dead blue cells were measured. The greater the number of inactive cells or cells with incomplete membranes, the deeper the trypan blue staining.

## RESULTS

### Identification and annotation of the *Hsp20* and *Hsf* genes in *B. distachyon*

The identification and evolution of *Hsf* genes has been explored in *B. distachyon* (Table 1; Yang et al., 2014), but the relationship between *Hsp20* and *Hsf* genes needs further investigation. To identify the *Hsp20* genes, we used their sequences from *A. thaliana* and *O. sativa* as queries for BLASTP analyses in the *B. distachyon* genome database. Ultimately, a total of 18 non-redundant *Hsp20* and 24 *Hsf* sequences were retrieved (Table 1). Moreover, the genes of *Hsp20* and *Hsf* in *B. distachyon* followed the same nomenclature rule as those of *A. thaliana* and *O. sativa* based on their sequence similarities and subcellular localization, particularly *BdHsp20s*. For example, *Bradi1g44230* was designated as *BdHsp15.8-PX* according to its subcellular peroxisomal (PX) localization and Mw of 15.8 kD (Table 1). The results showed that most of the *BdHsp*s (11) were located at the cytoplasm (C), except for three *BdHsp*s in the endoplasmic reticulum, one in the PX, one in the chloroplast (CP), and two in the mitochondria (M) (Table 1). Additionally, the protein size of all *BdHsp20* proteins varied from 144aa (*BdHsp15.8-PX*) to 364aa (*BdHsp40.0-M*), while *BdHsf* proteins ranged from 248aa (*BdHsfC1b*) to 649aa (*BdHsfA6a*) (Table 1). Furthermore, *BdHsp20s* possessed one intron or were intronless, while all *BdHsfs*, except *BdHsfA6a* (4) and *BdHsfA1a* (2), contained one intron (Table 1). The pI of *BdHsp20* proteins ranged from 4.78 (*BdHsp18.7-CI*) to 8.86 (*BdHsp40.0-M*) and the acidic proteins dominated, while the *BdHsf* proteins varied from 4.69 (*BdHsfA2a*) to 9.82 (*BdHsfB1a*) with the acidic proteins also occupying the main points (Table 1).

### Phylogenetic classification and gene structure of *BdHsp20s* and *BdHsfs*

To evaluate the evolutionary relationship between *BdHsp20s* and *BdHsfs*, the phylogenetic tree was independently reconstructed based on the sequence alignments of *B. distachyon*, *A. thaliana*, and *O. sativa* full-length amino acids (Table S4) and using the ML method. According to our phylogenetic analysis and subcellular localization prediction results, the *BdHsp20s* could be divided into cytoplasmic (CI, CII, CIII, CIV, CV, and CVI), CP, ER, M, and PX subfamilies (Fig. 1A). Most *Hsp20s* belonged to the CI subfamily, suggesting that the cytoplasm may be the main functional region of the plant *Hsp20s*. The CVI subfamily had only one member and was derived from *A. thaliana*, while *B. distachyon* and *O. sativa* had no members (Fig. 1A), implying that CVI *Hsp20* might only exist in dicotyledons. We also found a close relationship between the M and CP subfamilies (Fig. 1A), which supports the results of a previous study (Waters, Aevermann & Sanders-Reed, 2008). It was interesting that the classification of subfamilies was closely consistent with the pattern of intron-exon structure, as supported by previous research (Ouyang et al., 2009).

Likewise, phylogenetic analysis divided *Hsfs* into three main clades, designated as classes A, B, and C (Fig. 1B). Class A *Hsfs* were further divided into nine groups based on their phylogenetic relationships: subgroup A1, A2, A3, A4, A5, A6, A7, A8, and A9. Of these nine groups, most of the subgroups contained genes in three plant genomes, except for subgroup A9 which was only in *A. thaliana* and subgroup A2 and A7 which were absent

**Table 1** Characteristics of *BdHsp20* and *BdHsf* gene families.

Gene Name	Locus ID	Orientation	ORF	No. of a.a	No. of introns	5'-3'Coordinate	pI	Mw(kD)
BdHsp16.8-CIV	Bradi1g26190	-	459	152	1	21279133-21279701	6.06	16.8
BdHsp15.8-PX	Bradi1g44230	+	435	144	0	42485161-42485595	6.92	15.8
BdHsp17.3-CI	Bradi1g53850	+	471	156	0	52437678-52438148	5.79	17.3
BdHsp16.9-CI	Bradi1g67040	+	456	151	0	65991938-65992393	5.98	16.9
BdHsp17.6-CI	Bradi1g67080	+	477	158	1	66023992-66024468	5.98	17.6
BdHsp18.7-CI	Bradi2g02350	+	537	178	1	1609756-1610292	4.78	18.7
BdHsp17.2A-CI	Bradi2g02400	-	465	154	0	1631165-1631629	6.76	17.2
BdHsp17.2B-CI	Bradi2g02410	+	462	153	0	1632105-1632566	6.19	17.2
BdHsp18.0-CII	Bradi2g05374	-	498	165	0	3913040-3913537	5.96	18
BdHsp16.4-CI	Bradi2g12990	+	444	147	0	11414902-11415345	6.19	16.4
BdHsp20.5-ER	Bradi3g02710	-	585	341	0	1675529-1676113	7.94	20.5
BdHsp22.0-ER	Bradi4g21070	+	615	204	0	24169313-24169927	6.25	22
BdHsp24.2-ER	Bradi5g11110	-	657	218	0	14808972-14809628	5.52	24.2
BdHsp18.3-CIII	Bradi3g60100	+	510	169	1	58879440-58880020	6.59	18.3
BdHsp26.4-CP	Bradi1g68440	+	720	239	1	67159967-67160773	6.77	26.4
BdHsp23.2-M	Bradi3g58590	-	642	213	1	57826850-57827614	7.9	23.2
BdHsp21.0-CV	Bradi2g20767	-	570	189	1	18240585-18242132	4.84	21
BdHsp40.0-M	Bradi3g07421	-	1095	364	1	57826850-57827614	8.86	40
BdHsfA1a	Bradi1g01130	+	1866	622	2	758757-763160	4.92	67.716
BdHsfA2a	Bradi1g37720	-	1047	349	1	33623352-33624526	4.69	38.014
BdHsfA2b	Bradi2g41530	+	1143	381	1	41768002-41770456	5.94	42.777
BdHsfA3a	Bradi3g44700	-	1536	512	1	46678418-46681158	5.52	56.011
BdHsfA4a	Bradi2g49860	+	1317	439	1	49859988-49861908	5.39	48.86
BdHsfA5a	Bradi2g18980	-	1095	365	1	16735799-16737098	5.38	40.652
BdHsfA5b	Bradi3g43710	+	1407	469	1	45299059-45301814	4.93	51.677
BdHsfA6a	Bradi1g08891	+	1947	649	4	6281780-6283033	6.43	70.343
BdHsfA6b	Bradi1g74350	-	1020	340	1	71592465-71594730	5.25	38.841
BdHsfA6c	Bradi3g26920	-	1071	357	1	27700103-27702438	5.16	40.236
BdHsfA7a	Bradi1g05550	-	1044	348	1	3777047-3779557	5.5	39.021
BdHsfA7b	Bradi1g55630	-	1374	458	1	54141088-54143900	4.88	50.304
BdHsfA8a	Bradi1g69407	-	1182	394	1	67838063-67840368	4.83	43.389
BdHsfB1a	Bradi4g32130	+	909	303	1	37847110-37850047	9.82	32.79
BdHsfB2a	Bradi3g42130	-	1038	346	1	43857313-43858451	8.1	36.641
BdHsfB2b	Bradi4g35780	-	1200	400	1	41115331-41116660	5.05	41.873
BdHsfB3a	Bradi5g18680	+	924	308	1	21774260-21775269	5.29	32.975
BdHsfB4a	Bradi1g19900	-	942	314	1	15943892-15946059	6.68	34.736
BdHsfB4b	Bradi1g61620	+	840	280	1	60967400-60969034	6.15	31.752
BdHsfB4c	Bradi4g32050	-	1215	405	1	37779303-37780616	8.97	42.982
BdHsfC1a	Bradi2g44050	+	1008	336	1	44543658-44544857	5.23	36.787
BdHsfC1b	Bradi2g48990	+	744	248	1	49157232-49158080	9.07	26.933
BdHsfC2a	Bradi1g38140	+	759	253	1	34296765-34297648	6.11	26.937
BdHsfC2b	Bradi3g08870	+	945	315	1	6966950-6968174	6	33.332

**Notes.**

C, Cytoplasmic; CP, Chloroplast; ER, endoplasmic reticulum; M, Mitochondrial and PX, peroxisomal.

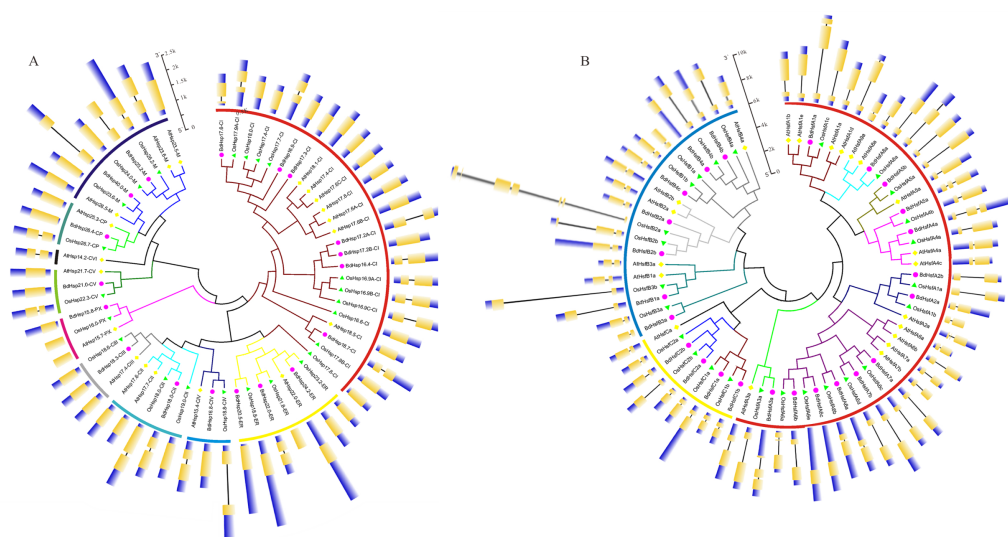


**Figure 1** Phylogenetic relationships and gene structure analysis of Hsf (A) and Hsp20 (B) genes from *O. sativa*, *A. thaliana*, and *B. distachyon*, respectively.

Full-size DOI: [10.7717/peerj.12267/fig-1](https://doi.org/10.7717/peerj.12267/fig-1)

in *O. sativa* (Fig. 1B). Moreover, class B was divided into four subgroups (B1, B2, B3, and B4), while class C Hsfs were separated into C1 and C2. It was notable that there was only one member in *A. thaliana*, while class C Hsfs were amplified in *B. distachyon* and *O. sativa* (Fig. 1B), indicating that these multiple gene copies may exhibit expansion in monocots. Furthermore, we also found that the subgroup classification patterns were related to intron-exon organization, e.g., class C Hsfs had fully similar intron numbers, exon lengths, and intron phases (Fig. 1B).

### Chromosomal location and gene duplication of *BdHsp20s* and *BdHsfs*

To analyze the relationship between the gene duplication and genetic divergence within *BdHsp20s* or *BdHsfs*, we investigated their chromosomal locations based on the information from the PLAZA database. The physical locations and CpG island distributions of the *BdHsp20* and *BdHsf* genes on *B. distachyon* chromosomes were drawn (Fig. 2). The results showed that the 18 *BdHsp20s* and 24 *BdHsfs* were mapped on five *B. distachyon* chromosomes: 16 genes were located on chromosome 1, 11 genes on chromosome 2, nine genes on chromosome 3, four genes on chromosome 4, and only one Hsf and Hsp20 member on chromosome 5 (Fig. 2). Interestingly, all *BdHsp20* and *BdHsf* gene members were encoded at the low-density region of CpG islands on all five chromosomes, suggesting that the expression of these genes may be regulated by other genes, which was consistent with previous studies (Bird, 1986; Hahn et al., 2011).

Gene duplication events, such as tandem duplication and segmental duplication, might generate new members of a gene family because of the important role that base substitution, deletion, and insertion into different chromosomes play in the expansion of gene families (Cannon et al., 2004). Therefore, we surveyed the duplication events of *BdHsp20s* and

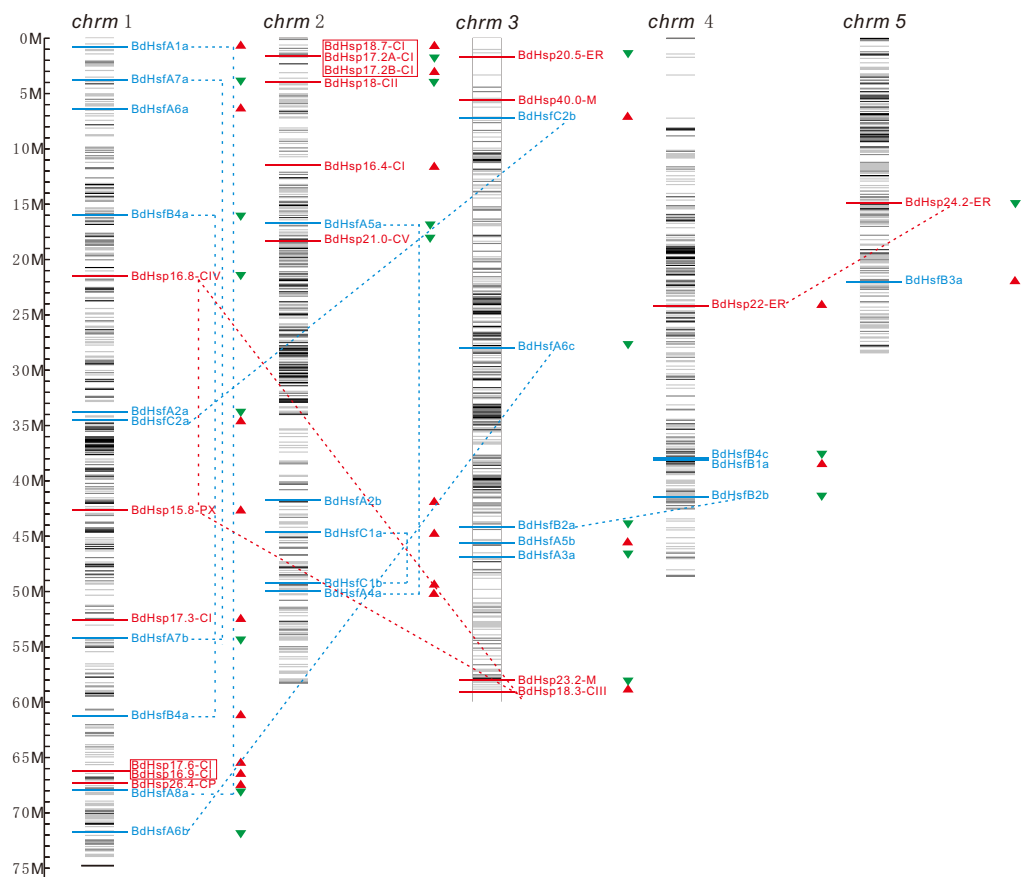


**Figure 2** Chromosomal location and gene duplication analyses for *B. distachyon* *Hsp20* and *Hsf* genes. The chromosomal position of each *BdHsf* and *BdHsp20* gene was mapped according to the *B. distachyon* genome. The chromosome number is indicated at the top of each chromosome. The CpG island distribution maps shown in each chromosome depended on the CpG density in the *B. distachyon* genome. The colored lines and characters represent the subgroup to which proteins in each clade belong. The dotted line shows the gene duplication events across these *BdHsf* and *BdHsp20* genes. The scale bar is shown on the left.

Full-size DOI: 10.7717/peerj.12267/fig-2

*BdHsf*s. We found that five pairs of duplicates underwent tandem duplication and 12 pairs of gene duplicates underwent segmental duplication (Fig. 2), indicating that tandem duplication and segmental duplication might contribute to the amplification of these gene families. These results showed that the greater number of gene family members might be the result of genomic rearrangement and expansion during the evolution process.

### Protein structure and tissue-specific expression profile of *BdHsp20*s and *BdHsf*s

To better understand *BdHsp20* and *BdHsf* characteristics, we further analyzed their sequence features, specifically the ACD of *BdHsp20*s and the HR-A/B of *BdHsf*s (Fig. 3A and 3B). As expected, all *BdHsp20*s contained an ACD consensus sequence that was composed of two regions: CRI and CRII (Fig. 3A). CRI was formed by  $\beta 2$ ,  $\beta 3$ ,  $\beta 4$ , and  $\beta 5$ , while CRII was formed by  $\beta 6$ ,  $\beta 7$ ,  $\beta 8$ , and  $\beta 9$ . However, *BdHsp16.8-CIV* and



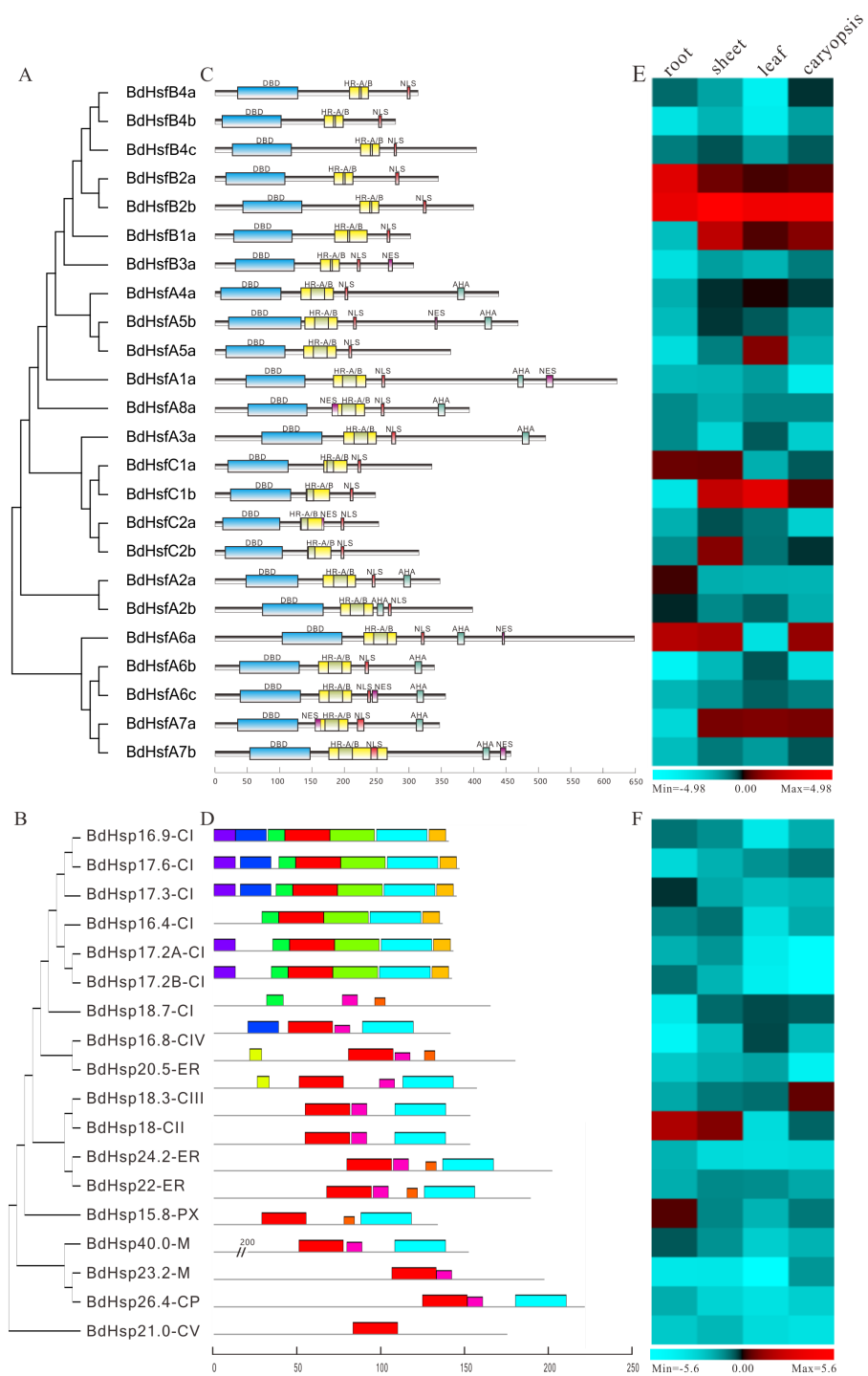


**Figure 4** Phylogenetic relationships and protein structure analysis of BdHsf and BdHsp20 proteins with tissue-specific expression profiles. (A–B) The phylogenetic tree was constructed from the amino acid sequences using the ML program from MEGA 5, and represents relationships between BdHsf and BdHsp20 proteins. (C–D) Domain analysis of BdHsf and BdHsp20 proteins. (E–F) Expression patterns of *BdHsf* and *BdHsp20* genes in different tissues including root, shoot, leaf, and caryopsis, respectively.

Full-size [DOI: 10.7717/peerj.12267/fig-4](https://doi.org/10.7717/peerj.12267/fig-4)

domain, which was composed of a CRI region ( $\beta 2$ ,  $\beta 3$ ,  $\beta 4$ , and  $\beta 5$ ) formed by motif 1 and motif 4, and a CRII region ( $\beta 6$ ,  $\beta 7$ ,  $\beta 8$ , and  $\beta 9$ ) formed by motif 2 and motif 3 (Fig. S1). Interestingly, the clustered *BdHsp20* pairs localizing the same cellular compartments also exhibited highly similar motif organization, such as *BdHsp18.3-CIII/BdHsp18-CII* and *BdHsp24.2-ER/BdHsp22-ER* (Fig. 4D), indicating that the protein architecture was helpful in the distribution and aggregation of the protein.

We also investigated the expression patterns of *BdHsf* and *BdHsp20* genes in four tissues or organs (root, shoot, leaf, and caryopsis) using the RT-qPCR method. We found that *BdHsfB2a* and *BdHsfB2b* were highly expressed in four tissues; *BdHsfB1a*, *BdHsfC1b*, and *BdHsfA7a* had a relatively high expression level in all tissues except for root; and *BdHsfA6a* was highly expressed in root, shoot, and caryopsis (Fig. 4E). Other *BdHsf* genes displayed a relatively low expression level in all tissues (Fig. 4E). Additionally, most *BdHsp20* gene members also showed low expression in all tissues, except for a few genes with moderate or high expression levels (Fig. 4F). For example, *BdHsp18-CII* showed high expression in root and shoot, *BdHsp18.3-CIII* showed high expression in caryopsis, and *BdHsp17.3-CI* and *BdHsp15.8-PX* were moderately expressed in the root (Fig. 4F). These results suggested that *BdHsf* and *BdHsp20* genes may not be expressed during normal growth and development, but are rapidly and highly expressed in response to stresses.

### Cis-elements and expression analysis of *BdHsp20s* and *BdHsfs* under multiple abiotic stresses and ABA treatment

To explore the function of *BdHsp20s*' and *BdHsfs*' response to abiotic stresses and hormones, the Bd21 seedling expression profiles were examined using RT-qPCR under dark, heat, UV-B, and ABA treatments. We first investigated the cis-elements in the -2 kb promoter region of the *BdHsf* and *BdHsp20* genes, except for *BdHsp17.2A-CI*, *BdHsp17.2B-CI*, and *BdHsp40.0-M* on account of their lack of a promoter region. The clustering result was obtained based on the phylogenetic tree of the full-length CDS sequence (Fig. 5A and 5B). We found that *BdHsp20s* and *BdHsfs* contained various cis-elements involved with defense and hormone and stress responsiveness (Fig. 5C and 5D). For instance, almost all *BdHsf* genes had G-Box and MBS elements, while most genes lacked motif IIb, ERE, and TCA-element 2, even all TATC-box and CE I (Table S5), suggesting that *BdHsf* genes may be mainly induced by abiotic stresses, not hormones. Likewise, only one *BdHsp20* gene member contained one cis-element including TATC-box, TCA-element 2, CE I, and motif IIb which associated with hormone response, while most *BdHsp20* gene members contained ARE and MBS elements (Table S5). Most importantly, seven *BdHsp20* genes (*BdHsp16.8-CIV*, *BdHsp15.8-PX*, *BdHsp17.3-CI*, *BdHsp24.2-ER*, *BdHsp18.3-CIII*, *BdHsp26.4-CP*, and *BdHsp21.0-CV*) contained HSE elements (Table S5).

We then investigated the transcript levels of *BdHsp20s* and *BdHsfs* under multiple abiotic stresses and ABA treatment. The results showed that most *BdHsp20s* and *BdHsfs*, such as *BdHsfA3a*, were strongly induced by heat stress, were moderately regulated by dark treatment, and were almost not affected by ABA and UV-B treatments (Fig. 5E and 5F). However, there were some differences in the expression profiles of some genes. For example, the expression levels of *BdHsfA6a* and *BdHsfA5b* significantly increased after ABA

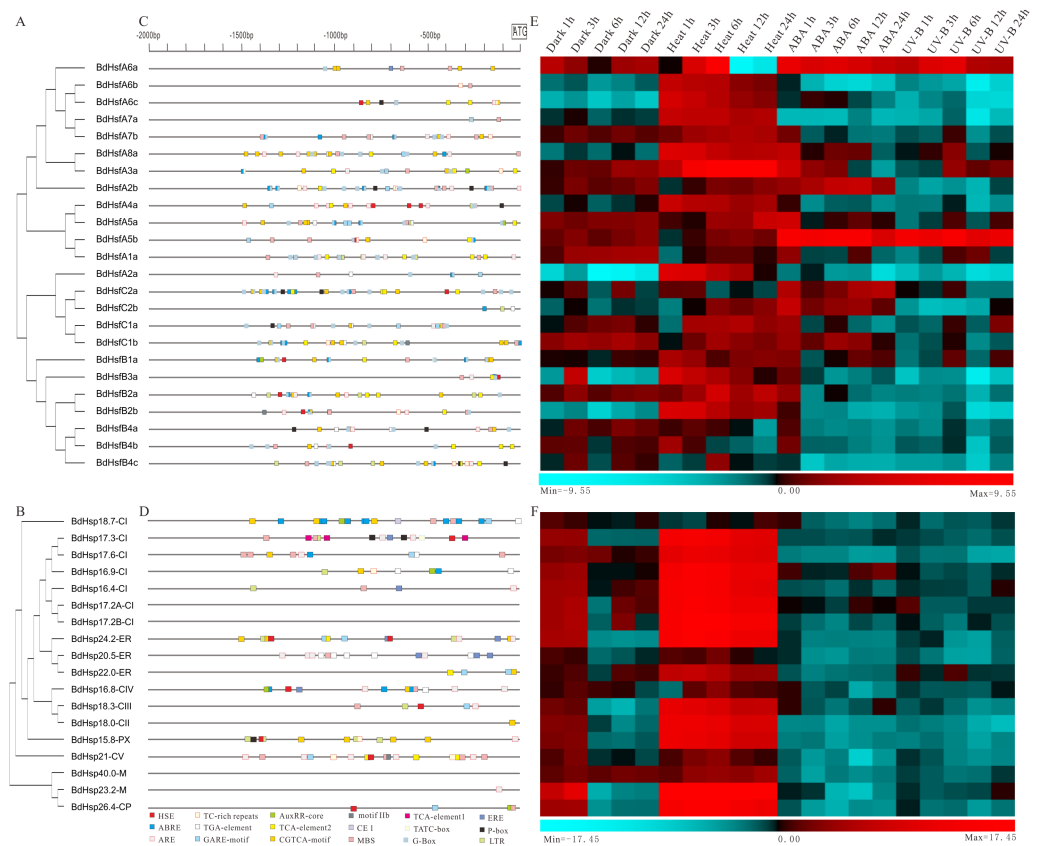


**Figure 5** Phylogenetic relationships and cis-element analysis with expression profiles of *BdHsf* and *BdHsp20* genes under different abiotic stresses. (A–B) The phylogenetic tree was constructed from the CDS sequences using the ML program from MEGA 5, and represents relationships between *BdHsf* and *BdHsp20* genes. (C–D) Promoter analysis of *BdHsf* and *BdHsp20* genes. All promoter sequences (–2000 bp) were analyzed. The scale bar at the top indicates the length of the promoter sequence. (E–F) Expression patterns of *BdHsf* and *BdHsp20* genes under different abiotic stresses including dark, heat, ABA, and UV-B treatments.

Full-size [DOI: 10.7717/peerj.12267/fig-5](https://doi.org/10.7717/peerj.12267/fig-5)

and UV-B treatments, while *BdHsfA2b* increased in the ABA condition (Fig. 5E), which was consistent with their corresponding cis-element distributions. The expression levels of *BdHsfA6a* were up-regulated after heat stress, peaking at 6 h, and then recovered to relatively low levels (Fig. 5E and Table S6). Interestingly, many *BdHsp20* genes (including *BdHsp23.2-M* and *BdHsp26.4-CP*) showed growth under early dark treatment, peaking at 3 h, and then dropping to very low levels (Fig. 5F). Heat stress had no obvious influence on the expression of *BdHsp18.7-CI*, *BdHsp20.5-ER*, and *BdHsp16.8-CIV*, which may be due to their missing HSE element (Fig. 5F and Table S6). These results indicated that *BdHsp20s* and *BdHsfs* were all strongly regulated by heat stress and regulated the expressions of downstream genes.

To further survey the potential factor of gene expression, we calculated the correlation coefficient between 3'UTR length and *BdHsp20* gene expression under heat stress. The result revealed that all of the *BdHsp20* genes had a significant negative correlation with their

3'UTR length (Fig. S2). The shorter 3'UTR length, the higher expression of *BdHsp20* genes under heat stress, which may be because of the escape from the inhibition of some miRNAs (Zhang *et al.*, 2019). However, under heat stress, the 5'UTR length had no significant effect on the expression of *BdHsp20* genes, which fully conflicted with the correlation of 3'UTR (Fig. S3). Even so, we found that the 5'UTR lengths showed a negative correlation with gene expression levels of *BdHsp20* genes under heat stress, which was in accordance with a previous study (Rao *et al.*, 2013).

### ***BdHsp20* and *BdHsf* gene regulatory network**

Together, Hsfs and Hsp20s usually formed signaling modules in response to environmental stresses, especially heat shock stimuli (Lin *et al.*, 2011). Hsp20 expression can be strongly induced by heat and other abiotic stresses, while Hsfs can initially perceive the stimuli and facilitate the expression of Hsps by binding to the HSE of the *Hsp* promoter region (Schoffl, Prandl & Reindl, 1998). To explore the potential regulatory network between *BdHsfs* and the downstream protein *BdHsp20s* under heat stress, we calculated the correlation coefficient between their expression results and constructed the correlation expression network (consisting of 111 nodes and 402 interactions) using Cytoscape software (Fig. 6). We selected the molecular modules if the values of their correlation coefficients were greater than 0.7. The results showed that eight *BdHsp20* genes (*BdHsp18-CII*, *BdHsp18.3-CIII*, *BdHsp15.8-PX*, *BdHsp17.3-CI*, *BdHsp40.0-M*, *BdHsp16.4-CI*, *BdHsp18.7-CI*, and *BdHsp16.8-CIV*) were regulated by almost all *BdHsf* genes (Fig. 6). For instance, the *BdHsp18-CII* gene could be regulated by 12 *BdHsf* genes, while *BdHsp15.8-PX* and *BdHsp18.3-CIII* could be regulated by 11 *BdHsf* genes (Fig. 6). Other *BdHsp20* genes might be regulated by other *BdHsf* genes under other abiotic stresses. Moreover, all *BdHsf* genes, except *BdHsfC2b*, could regulate more than one *BdHsp20* gene. For example, *BdHsfB4a* could regulate eleven *BdHsp20* genes (Fig. 6). Furthermore, it was notable that *BdHsfA5b* and *BdHsfA7b* expression showed significant negative correlation with *BdHsp20s*, suggesting that they may be transcriptional repressors. These results indicated a complex signaling regulatory network between *BdHsp20s* and *BdHsfs*, which may exhibit the same functions or interactions in response to heat stress treatment.

### ***BdHsp20* gene overexpression improved plant seed germination under heat stress**

To investigate the effect of high-temperature stress on *BdHsp20* seed germination, we examined the seed germination rate and trypan blue staining assays of heterologous expression in *A. thaliana* across five *BdHsp20* genes. We found that the germination rate of *BdHsp20* genes in transgenic plants was higher than in WT seedlings (Fig. 7 and Table S7). For example, the germination rate of *BdHsp17.2B-CI* transgenic plants was 69.5 after treatment, while WT seedlings showed a germination rate of 37 (Fig. 7 and Table S7). This finding indicated that *BdHsp20* transgenic plants had a higher survival rate under high-temperature stress. To further explore the details of cell survival under high-temperatures, the trypan blue staining of the leaf blade was executed. The results showed that the WT leaf was a deeper blue when compared to *BdHsp20* transgenic leaves

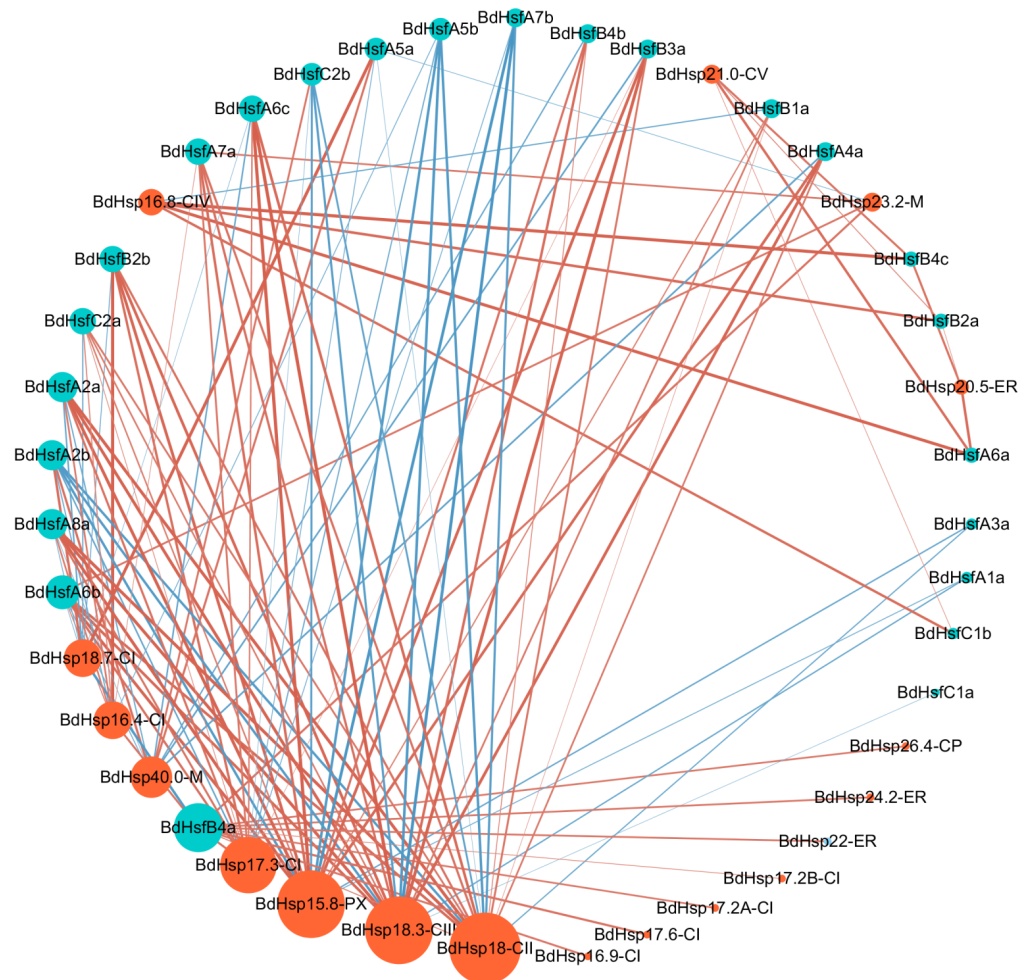


**Figure 6** Visualization for the predicted results of the expression network between *BdHsfs* and *BdHsp20s*, constructed using the Cytoscape tool. Each node represents a protein, and each line represents an interaction. The orange and blue node color indicates the *BdHsp20* and *BdHsf* gene families, respectively. Line thickness reflects the correlation strength of the expression. Font size and circle color indicate the correlated expression number. Our results showed that there were 143 pairs of potential expression pairs. The network was generated using the Cytoscape tool.

Full-size  DOI: [10.7717/peerj.12267/fig-6](https://doi.org/10.7717/peerj.12267/fig-6)

under high-temperature stress (Fig. 7), indicating that there was more cell death in WT plants. Therefore, we concluded that these *BdHsp20* genes can enhance resistance to heat stress.

## DISCUSSION

### Phylogeny, evolution, and duplication analyses of *BdsHsp20* and *BdHsf* gene families

In this study, we investigated the evolution of *BdsHsp20* and *BdHsf* gene families. We first retrieved 18 *sHsp20s* and 24 *Hsfs* in *B. distachyon* and then reconstructed their ML phylogenetic trees (Fig. 1). *B. distachyon* *BdHsfs* and *BdsHsp20s* were divided into three

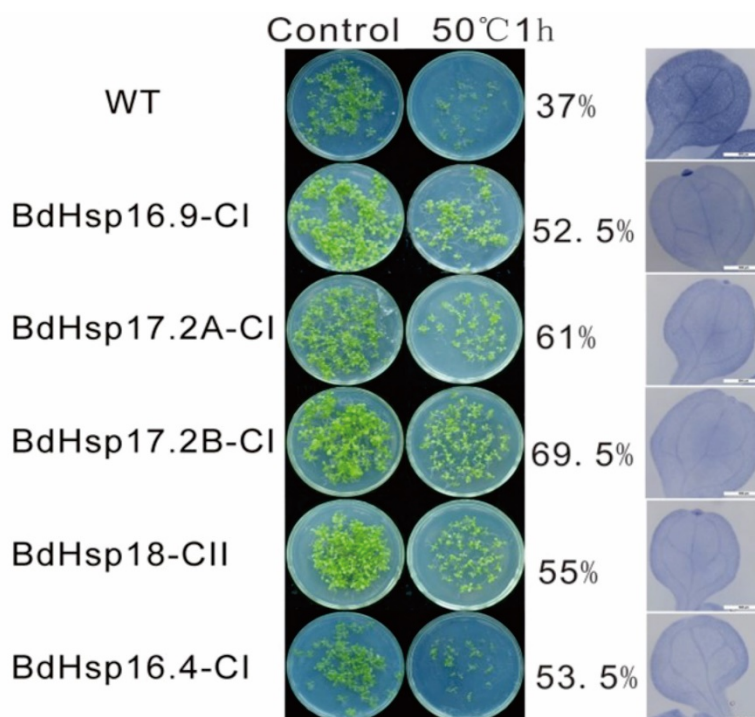


**Figure 7** The effect of BdHsp20 overexpression on seed germination and leaf cell death after heat treatment.

Full-size DOI: [10.7717/peerj.12267/fig-7](https://doi.org/10.7717/peerj.12267/fig-7)

and ten subfamilies, respectively (Fig. 1), similar to *A. thaliana* and rice (Scharf *et al.*, 2012). Further analysis showed that the pattern of *BdsHsp20* and *BdHsf* gene families' intron-exon organization was closely related to their phylogenetic branch (Fig. 1). In addition, *BdHsp20s* and *BdHsfs* were all located in the low-density region of CpG islands, and were distributed tendentially on all five chromosomes (Fig. 2), which was in accordance with previous research (Jiang *et al.*, 2015). We also found that four pairs of duplicates showed tandem duplication in subgroup CI *BdsHsp20s* (Fig. 2), suggesting that tandem duplication contributed to the expansion of these genes, similar to the patterns of the *MKK* gene family (Jiang & Chu, 2018; Jiang, Li & Wang, 2021). Moreover, domain and 3D structure analyses showed that *BdHsp20s* and *BdHsfs* were highly conserved (Fig. 3). Most importantly, these results indicated that the *BdsHsp20* and *BdHsf* gene families were highly conserved.

### Correlation regulatory networks across *BdHsp20* and *BdHsf* genes

Numerous *Hsp* and *Hsf* genes have been reported in higher plants such as *Prunus mume* (Wan *et al.*, 2019) and *Populus trichocarpa* (Zhang *et al.*, 2015). It is well-known that tissue-specific expression patterns may enable *Hsp* and *Hsf* proteins to have distinct functions in different signaling pathways, although *Hsp* and *Hsf* proteins usually show low abundance under normal conditions. For example, *PtHsf-A2* showed high transcript levels in internode 9, *PtHsf-B2a* showed high transcript levels in internode 5, and *PtHsf-A6a* showed high levels in female catkins, which was in accordance with a previous study that reported that these

genes are key regulators of downstream *Hsps* (Nishizawa *et al.*, 2006). Therefore, we examined the expression profiles of different tissues in *B. distachyon*. *BdHsfB2a* was highly expressed in four tissues, and *BdHsfA6a* in root, shoot, and caryopsis (Fig. 4E), implying that they might have a unique signaling pathway. Moreover, almost all *BdHsp20s* and *BdHsfs* were significantly up-regulated under heat stress (Fig. 5E), indicating that these genes play a significant role in heat stress response. Furthermore, correlation networks between *PtHsfs* and *PtHsps* under various stresses (Zhang *et al.*, 2015) and HSF/HSP with switchgrass Cd tolerance (Song *et al.*, 2018) have been constructed. In this study, *BdHsfB4a*, *BdHsfA5b* and *BdHsfA7b* revealed high correlation levels with *BdHsps* (Fig. 6), suggesting that these *BdHsfs* may be the key regulators for many *BdHsps*. On the other hand, several *BdHsp20s*, including *BdHsp18-CII*, *BdHsp18.3-CIII*, and *BdHsp15.8-PX*, displayed co-expression with *BdHsfs* (Fig. 6), indicating that these genes might play a crucial role in the heat stress response. However, the regulatory mechanisms of herbaceous Hsf and sHsp plant growth, development, and stress responses require further study.

### Functional analysis of *BdHsp20s* in *B. distachyon* under high temperatures

Previous studies suggested that *VcHSP17.7* was associated with the chilling injury resistance of blueberry (*Vaccinium corymbosum*) fruit induced by heat shock treatment (Shi *et al.*, 2017). *Rosa chinensis RcHsp17.8* confers stress tolerance to heat, cold, salt, drought, and osmotic and oxidative conditions (Jiang *et al.*, 2009), while *OsHSP18.6* overexpression improved thermotolerance (Wang *et al.*, 2015). In this study, *BdHsp17.2B-CI* expression was strongly up-regulated under heat conditions (Fig. 5), whereas overexpression in *A. thaliana* plants enhanced their tolerance to heat stress by decreasing cell death (Fig. 7), indicating that *BdHsp17.2B-CI* conferred resistance to heat stress. Similarly, *AtHSP17.4* and *CsHSP17.2* were also more actively expressed in transgenic overexpressed plants under heat shock (Wahid *et al.*, 2007; Wang *et al.*, 2017). The rest of the four overexpressed *BdHsp20s* in *A. thaliana* also showed improved tolerance to heat stress (Fig. 7), which supported previous transgenic research (Guo *et al.*, 2020). The heterologous expression of *LimHSP16.45* in Arabidopsis enhanced their tolerance to various stresses by forming heat shock particles (HSGs) (Mu *et al.*, 2013). Although it is well-known that *HSP20* genes can be induced by heat stress, some heat-regulated genes were almost expressed or downregulated under UA-B and/or dark conditions (Fig. 5F), suggesting that *HSP20* genes may have a negative or only slight effect under UA-B and/or dark stress. These results suggest that the signaling pathways may be different in a plant's response to heat and light stress. Collectively, these results provide a basis for further functional research on the roles of these families in herbaceous plant stress responses.

## CONCLUSION

In this study, we retrieved 24 *Hsf* and 18 *sHsp* genes in *B. distachyon* using bioinformatics approaches. Based on the phylogenetic tree, subcellular localization, and domain analyses, the *BdHsfs* were categorized into three classes, and the *BdHsp20s* were divided into ten subfamilies. Notably, we found that 3'UTR length might negatively affect *BdHsp20* gene

expression. Expression analysis showed that most *BdHsp20s* and *BdHsfs* were strongly and rapidly regulated by heat stimuli, moderately induced by dark treatment, and almost not affected at all by ABA and UV-B treatments. More importantly, the correlation regulatory network between *BdHsp20s* and *BdHsfs* under heat stress treatments showed a complex signaling regulatory network. Additionally, seed germination and trypan blue staining analyses revealed that *BdHsp20s* enhanced high-temperature tolerance. These results provide useful information for future research on the regulatory networks of *BdHsp20s*' and *BdHsfs*' response to environmental stresses, and improved our understanding of the functions of *Hsf* and *sHsp* genes in herbaceous plants.

## ADDITIONAL INFORMATION AND DECLARATIONS

### Funding

This work was funded by a grant from the Shanghai Sailing Program (19YF1414800). The funders had no role in study design, data collection and analysis, decision to publish, or preparation of the manuscript.

### Grant Disclosures

The following grant information was disclosed by the authors:  
Shanghai Sailing Program: 19YF1414800.

### Competing Interests

The authors declare there are no competing interests.

### Author Contributions

- Na Li conceived and designed the experiments, performed the experiments, analyzed the data, prepared figures and/or tables, authored or reviewed drafts of the paper, and approved the final draft.
- Min Jiang conceived and designed the experiments, performed the experiments, analyzed the data, prepared figures and/or tables, authored or reviewed drafts of the paper, and approved the final draft.
- Peng Li and Xiwen Li analyzed the data, prepared figures and/or tables, and approved the final draft.

### Data Availability

The following information was supplied regarding data availability:

The data of RT-qPCR experiments are available in the [Supplemental Table](#).

### Supplemental Information

Supplemental information for this article can be found online at <http://dx.doi.org/10.7717/peerj.12267#supplemental-information>.

## REFERENCES

- Bailey TL, Johnson J, Grant CE, Noble WS. 2015. The MEME suite. *Nucleic Acids Research* 43:W39–W49 DOI 10.1093/nar/gkv416.
- Bird AP. 1986. CpG-rich islands and the function of DNA methylation. *Nature* 321:209–213 DOI 10.1038/321209a0.
- Bondino HG, Valle EM, Ten Have A. 2012. Evolution and functional diversification of the small heat shock protein/alpha-crystallin family in higher plants. *Planta* 235:1299–1313 DOI 10.1007/s00425-011-1575-9.
- Cannon SB, Mitra A, Baumgarten A, Young ND, May G. 2004. The roles of segmental and tandem gene duplication in the evolution of large gene families in *Arabidopsis thaliana*. *BMC Plant Biology* 4:10 DOI 10.1186/1471-2229-4-10.
- Catalan P, Chalhoub B, Chochois V, Garvin DF, Hasterok R, Manzaneda AJ, Mur LA, Pecchioni N, Rasmussen SK, Vogel JP, Voxeur A. 2014. Update on the genomics and basic biology of Brachypodium: International Brachypodium Initiative (IBI). *Trends in Plant Science* 19:414–418.
- Cui J, Jiang N, Zhou X, Hou X, Yang G, Meng J, Luan Y. 2018. Tomato MYB49 enhances resistance to *Phytophthora infestans* and tolerance to water deficit and salt stress. *Planta* 248:1487–1503 DOI 10.1007/s00425-018-2987-6.
- Garvin DF, Gu YQ, Hasterok R, Hazen SP, Jenkins G, Mockler TC, Mur LAJ, Vogel JP. 2008. Development of genetic and genomic research resources for *Brachypodium distachyon*. A new model system for grass crop research. *Crop Science* 48:S69–S84 DOI 10.2135/cropsci2007.04.0208.
- Giorno F, Wolters-Arts M, Grillo S, Scharf KD, Vriezen WH, Mariani C. 2010. Developmental and heat stress-regulated expression of HsfA2 and small heat shock proteins in tomato anthers. *Journal of Experimental Botany* 61:453–462 DOI 10.1093/jxb/erp316.
- Guo LM, Li J, He J, Liu H, Zhang HM. 2020. A class I cytosolic HSP20 of rice enhances heat and salt tolerance in different organisms. *Scientific Reports* 10:1383 DOI 10.1038/s41598-020-58395-8.
- Guo J, Wu J, Ji Q, Wang C, Luo L, Yuan Y, Wang Y, Wang J. 2008. Genome-wide analysis of heat shock transcription factor families in rice and Arabidopsis. *Journal of Genetics and Genomics* 35:105–118 DOI 10.1016/S1673-8527(08)60016-8.
- Hahn MA, Wu X, Li AX, Hahn T, Pfeifer GP. 2011. Relationship between gene body DNA methylation and intragenic H3K9me3 and H3K36me3 chromatin marks. *PLOS ONE* 6:e18844 DOI 10.1371/journal.pone.0018844.
- Hartl FU, Bracher A, Hayer-Hartl M. 2011. Molecular chaperones in protein folding and proteostasis. *Nature* 475:324–332 DOI 10.1038/nature10317.
- Hu B, Jin J, Guo AY, Zhang H, Luo J, Gao G. 2015. GSDS 2.0: an upgraded gene feature visualization server. *Bioinformatics* 31:1296–1297 DOI 10.1093/bioinformatics/btu817.
- Hwang SM, Kim DW, Woo MS, Jeong HS, Son YS, Akhter S, Choi GJ, Bahk JD. 2014. Functional characterization of Arabidopsis HsfA6a as a heat-shock transcription

- factor under high salinity and dehydration conditions. *Plant Cell and Environment* **37**:1202–1222 DOI [10.1111/pce.12228](https://doi.org/10.1111/pce.12228).
- International Brachypodium I.** 2010. Genome sequencing and analysis of the model grass *Brachypodium distachyon*. *Nature* **463**:763–768 DOI [10.1038/nature08747](https://doi.org/10.1038/nature08747).
- Jiang M, Chu ZQ.** 2018. Comparative analysis of plant *MKK* gene family reveals novel expansion mechanism of the members and sheds new light on functional conservation. *BMC Genomics* **19**:407 DOI [10.1186/s12864-018-4793-8](https://doi.org/10.1186/s12864-018-4793-8).
- Jiang M, Li P, Wang W.** 2021. Comparative analysis of *MAPK* and *MKK* gene families reveals differential evolutionary patterns in *Brachypodium distachyon* inbred lines. *PeerJ* **9**:e11238 DOI [10.7717/peerj.11238](https://doi.org/10.7717/peerj.11238).
- Jiang M, Wen F, Cao J, Li P, She J, Chu Z.** 2015. Genome-wide exploration of the molecular evolution and regulatory network of mitogen-activated protein kinase cascades upon multiple stresses in *Brachypodium distachyon*. *BMC Genomics* **16**:228 DOI [10.1186/s12864-015-1452-1](https://doi.org/10.1186/s12864-015-1452-1).
- Jiang CH, Xu JY, Zhang H, Zhang X, Shi JL, Li M, Ming F.** 2009. A cytosolic class I small heat shock protein, RcHSP17.8, of *Rosa chinensis* confers resistance to a variety of stresses to *Escherichia coli*, yeast and *Arabidopsis thaliana*. *Plant Cell and Environment* **32**:1046–1059 DOI [10.1111/j.1365-3040.2009.01987.x](https://doi.org/10.1111/j.1365-3040.2009.01987.x).
- Kaur H, Petla BP, Kamble NU, Singh A, Rao V, Salvi P, Ghosh S, Majee M.** 2015. Differentially expressed seed aging responsive heat shock protein OsHSP18.2 implicates in seed vigor, longevity and improves germination and seedling establishment under abiotic stress. *Frontiers in Plant Science* **6**:713.
- Kotak S, Larkindale J, Lee U, Koskull-Doring Pvon, Vierling E, Scharf KD.** 2007. Complexity of the heat stress response in plants. *Current Opinion in Plant Biology* **10**:310–316 DOI [10.1016/j.pbi.2007.04.011](https://doi.org/10.1016/j.pbi.2007.04.011).
- Kriehuber T, Rattei T, Weinmaier T, Bepperling A, Haslbeck M, Buchner J.** 2010. Independent evolution of the core domain and its flanking sequences in small heat shock proteins. *FASEB Journal* **24**:3633–3642 DOI [10.1096/fj.10-156992](https://doi.org/10.1096/fj.10-156992).
- Krishna P, Sacco M, Cherutti JF, Hill S.** 1995. Cold-induced accumulation of hsp90 transcripts in *Brassica napus*. *Plant Physiology* **107**:915–923 DOI [10.1104/pp.107.3.915](https://doi.org/10.1104/pp.107.3.915).
- Lamesch P, Berardini TZ, Li D, Swarbreck D, Wilks C, Sasidharan R, Muller R, Dreher K, Alexander DL, Garcia-Hernandez M, Karthikeyan AS, Lee CH, Nelson WD, Ploetz L, Singh S, Wensel A, Huala E.** 2012. The Arabidopsis Information Resource (TAIR): improved gene annotation and new tools. *Nucleic Acids Research* **40**:D1202–D1210 DOI [10.1093/nar/gkr1090](https://doi.org/10.1093/nar/gkr1090).
- Lescot M, Dehais P, Thijs G, Marchal K, Moreau Y, VandePeer Y, Rouze P, Rombauts S.** 2002. PlantCARE, a database of plant cis-acting regulatory elements and a portal to tools for in silico analysis of promoter sequences. *Nucleic Acids Research* **30**:325–327 DOI [10.1093/nar/30.1.325](https://doi.org/10.1093/nar/30.1.325).
- Lin YX, Jiang HY, Chu ZX, Tang XL, Zhu SW, Cheng BJ.** 2011. Genome-wide identification, classification and analysis of heat shock transcription factor family in maize. *BMC Genomics* **12**:76 DOI [10.1186/1471-2164-12-76](https://doi.org/10.1186/1471-2164-12-76).

- Lindquist S, Craig EA. 1988. The heat-shock proteins. *Annual Review of Genetics* 22:631–677 DOI 10.1146/annurev.ge.22.120188.003215.
- Luan Y, Cui J, Li J, Jiang N, Liu P, Meng J. 2018. Effective enhancement of resistance to *Phytophthora infestans* by overexpression of miR172a and b in *Solanum lycopersicum*. *Planta* 247:127–138 DOI 10.1007/s00425-017-2773-x.
- Marrs KA, Casey ES, Capitant SA, Bouchard RA, Dietrich PS, Mettler IJ, Sinibaldi RM. 1993. Characterization of two maize HSP90 heat shock protein genes: expression during heat shock, embryogenesis, and pollen development. *Developmental Genetics* 14:27–41 DOI 10.1002/dvg.1020140105.
- Mayer MP, Bukau B. 2005. Hsp70 chaperones: cellular functions and molecular mechanism. *Cellular and Molecular Life Sciences* 62:670–684 DOI 10.1007/s00018-004-4464-6.
- Mitchell AL, Attwood TK, Babbitt PC, Blum M, Bork P, Bridge A, Brown SD, Chang HY, El-Gebali S, Fraser MI, Gough J, Haft DR, Huang H, Letunic I, Lopez R, Luciani A, Madeira F, Marchler-Bauer A, Mi H, Natale DA, Necci M, Nuka G, Orengo C, Pandurangan AP, Paysan-Lafosse T, Pesseat S, Potter SC, Qureshi MA, Rawlings ND, Redaschi N, Richardson LJ, Rivoire C, Salazar GA, Sangrador-Vegas A, Sigrist CJA, Sillitoe I, Sutton GG, Thanki N, Thomas PD, Tosatto SCE, Yong SY, Finn RD. 2019. InterPro in 2019: improving coverage, classification and access to protein sequence annotations. *Nucleic Acids Research* 47:D351–D360 DOI 10.1093/nar/gky1100.
- Mittler R. 2006. Abiotic stress, the field environment and stress combination. *Trends in Plant Science* 11:15–19 DOI 10.1016/j.tplants.2005.11.002.
- Mu C, Wang S, Zhang S, Pan J, Chen N, Li X, Wang Z, Liu H. 2011. Small heat shock protein LimHSP16.45 protects pollen mother cells and tapetal cells against extreme temperatures during late zygotene to pachytene stages of meiotic prophase I in David Lily. *Plant Cell Reports* 30:1981–1989 DOI 10.1007/s00299-011-1106-y.
- Mu C, Zhang S, Yu G, Chen N, Li X, Liu H. 2013. Overexpression of small heat shock protein LimHSP16.45 in Arabidopsis enhances tolerance to abiotic stresses. *PLOS ONE* 8:e82264 DOI 10.1371/journal.pone.0082264.
- Nishizawa A, Yabuta Y, Yoshida E, Maruta T, Yoshimura K, Shigeoka S. 2006. Arabidopsis heat shock transcription factor A2 as a key regulator in response to several types of environmental stress. *Plant Journal* 48:535–547 DOI 10.1111/j.1365-313X.2006.02889.x.
- Nover L, Bharti K, Doring P, Mishra SK, Ganguli A, Scharf KD. 2001. Arabidopsis and the heat stress transcription factor world: how many heat stress transcription factors do we need? *Cell Stress Chaperones* 6:177–189 DOI 10.1379/1466-1268(2001)006<0177:AATHST>2.0.CO;2.
- Ohama N, Kusakabe K, Mizoi J, Zhao H, Kidokoro S, Koizumi S, Takahashi F, Ishida T, Yanagisawa S, Shinozaki K, Yamaguchi-Shinozaki K. 2016. The transcriptional cascade in the heat stress response of Arabidopsis is strictly regulated at the level of transcription factor expression. *The Plant Cell* 28:181–201 DOI 10.1105/tpc.15.00435.

- Opanowicz M, Vain P, Draper J, Parker D, Doonan JH. 2008. Brachypodium distachyon: making hay with a wild grass. *Trends in Plant Science* 13:172–177 DOI 10.1016/j.tplants.2008.01.007.
- Ouyang Y, Chen J, Xie W, Wang L, Zhang Q. 2009. Comprehensive sequence and expression profile analysis of *Hsp20* gene family in rice. *Plant Mol Biol* 70:341–357 DOI 10.1007/s11103-009-9477-y.
- Ouyang S, Zhu W, Hamilton J, Lin H, Campbell M, Childs K, Thibaud-Nissen F, Malek RL, Lee Y, Zheng L, Orvis J, Haas B, Wortman J, Buell CR. 2007. The TIGR Rice Genome Annotation Resource: improvements and new features. *Nucleic Acids Research* 35:D883–D887 DOI 10.1093/nar/gkl976.
- Poulain P, Gelly JC, Flatters D. 2010. Detection and architecture of small heat shock protein monomers. *PLOS ONE* 5:e9990 DOI 10.1371/journal.pone.0009990.
- Qiao X, Li Q, Yin H, Qi K, Li L, Wang R, Zhang S, Paterson AH. 2019. Gene duplication and evolution in recurring polyploidization-diploidization cycles in plants. *Genome Biology* 20:38 DOI 10.1186/s13059-019-1650-2.
- Rao YS, Wang ZF, Chai XW, Nie QH, Zhang XQ. 2013. Relationship between 5' UTR length and gene expression pattern in chicken. *Genetica* 141:311–318 DOI 10.1007/s10709-013-9730-9.
- Sarkar NK, Kim YK, Grover A. 2009. Rice *sHsp* genes: genomic organization and expression profiling under stress and development. *BMC Genomics* 10:393 DOI 10.1186/1471-2164-10-393.
- Scharf KD, Berberich T, Ebersberger I, Nover L. 2012. The plant heat stress transcription factor (Hsf) family: structure, function and evolution. *Biochimica Et Biophysica Acta/General Subjects* 1819:104–119.
- Scharf KD, Rose S, Zott W, Schoffl F, Nover L. 1990. Three tomato genes code for heat stress transcription factors with a region of remarkable homology to the DNA-binding domain of the yeast HSF. *The EMBO Journal* 9:4495–4501 DOI 10.1002/j.1460-2075.1990.tb07900.x.
- Scharf KD, Siddique M, Vierling E. 2001. The expanding family of *Arabidopsis thaliana* small heat stress proteins and a new family of proteins containing alpha-crystallin domains (Acid proteins). *Cell Stress Chaperones* 6:225–237 DOI 10.1379/1466-1268(2001)006<0225:TEFOAT>2.0.CO;2.
- Schirmer EC, Lindquist S, Vierling E. 1994. An *Arabidopsis* heat shock protein complements a thermotolerance defect in yeast. *The Plant Cell* 6:1899–1909.
- Schoffl F, Prandl R, Reindl A. 1998. Regulation of the heat-shock response. *Plant Physiology* 117:1135–1141 DOI 10.1104/pp.117.4.1135.
- Shannon P, Markiel A, Ozier O, Baliga NS, Wang JT, Ramage D, Amin N, Schwikowski B, Ideker T. 2003. Cytoscape: a software environment for integrated models of biomolecular interaction networks. *Genome Research* 13:2498–2504 DOI 10.1101/gr.1239303.
- Shi WJ, Su SC, Li BB, Yang JF, Gong ZZ, Hou ZX. 2017. Molecular characterisation and expression analysis of a *sHSP* gene involved in heat shock treatment-induced chilling

- tolerance in highbush blueberry fruit. *Journal of Horticultural Science & Biotechnology* **92**:455–464 DOI [10.1080/14620316.2017.1304167](https://doi.org/10.1080/14620316.2017.1304167).
- Siddique M, Gernhard S, Koskull-Doring Pvon, Vierling E, Scharf KD. 2008.** The plant sHSP superfamily: five new members in *Arabidopsis thaliana* with unexpected properties. *Cell Stress Chaperones* **13**:183–197 DOI [10.1007/s12192-008-0032-6](https://doi.org/10.1007/s12192-008-0032-6).
- Song G, Yuan SX, Wen XH, Xie ZI, Lou LQ, Hu BY, Cai QS, Xu B. 2018.** Transcriptome analysis of Cd-treated switchgrass root revealed novel transcripts and the importance of HSF/HSP network in switchgrass Cd tolerance. *Plant Cell Reports* **37**:1485–1497 DOI [10.1007/s00299-018-2318-1](https://doi.org/10.1007/s00299-018-2318-1).
- Srivastava AK, Lu Y, Zinta G, Lang Z, Zhu JK. 2018.** UTR-dependent control of gene expression in plants. *Trends in Plant Science* **23**:248–259 DOI [10.1016/j.tplants.2017.11.003](https://doi.org/10.1016/j.tplants.2017.11.003).
- Sun Y, Macrae TH. 2005.** Small heat shock proteins: molecular structure and chaperone function. *Cellular & Molecular Life Sciences* **62**:2460–2476 DOI [10.1007/s00018-005-5190-4](https://doi.org/10.1007/s00018-005-5190-4).
- Tamura K, Peterson D, Peterson N, Stecher G, Nei M, Kumar S. 2011.** MEGA5: molecular evolutionary genetics analysis using maximum likelihood, evolutionary distance, and maximum parsimony methods. *Molecular Biology and Evolution* **28**:2731–2739 DOI [10.1093/molbev/msr121](https://doi.org/10.1093/molbev/msr121).
- Van Bel M, Diels T, Vancaester E, Kreft L, Botzki A, VandePeer Y, Coppens F, Vandepoele K. 2018.** PLAZA 4.0: an integrative resource for functional, evolutionary and comparative plant genomics. *Nucleic Acids Research* **46**:D1190–D1196 DOI [10.1093/nar/gkx1002](https://doi.org/10.1093/nar/gkx1002).
- Wahid A, Gelani S, Ashraf M, Foolad MR. 2007.** Heat tolerance in plants: an overview. *Environmental and Experimental Botany* **61**:199–223 DOI [10.1016/j.envexpbot.2007.05.011](https://doi.org/10.1016/j.envexpbot.2007.05.011).
- Wan X, Yang J, Guo C, Bao M, Zhang J. 2019.** Genome-wide identification and classification of the *Hsf* and *sHsp* gene families in *Prunus mume*, and transcriptional analysis under heat stress. *PeerJ* **7**:e7312 DOI [10.7717/peerj.7312](https://doi.org/10.7717/peerj.7312).
- Wang N, Liu W, Yu L, Guo Z, Chen Z, Jiang S, Xu H, Fang H, Wang Y, Zhang Z, Chen X. 2020.** HEAT SHOCK FACTOR A8a modulates flavonoid synthesis and drought tolerance. *Plant Physiology* **184**:1273–1290 DOI [10.1104/pp.20.01106](https://doi.org/10.1104/pp.20.01106).
- Wang W, Vinocur B, Altman A. 2003.** Plant responses to drought, salinity and extreme temperatures: towards genetic engineering for stress tolerance. *Planta* **218**:1–14 DOI [10.1007/s00425-003-1105-5](https://doi.org/10.1007/s00425-003-1105-5).
- Wang W, Vinocur B, Shoseyov O, Altman A. 2004.** Role of plant heat-shock proteins and molecular chaperones in the abiotic stress response. *Trends in Plant Science* **9**:244–252 DOI [10.1016/j.tplants.2004.03.006](https://doi.org/10.1016/j.tplants.2004.03.006).
- Wang AQ, Yu XH, Mao Y, Liu Y, Liu GQ, Liu YS, Niu XL. 2015.** Overexpression of a small heat-shock-protein gene enhances tolerance to abiotic stresses in rice. *Plant Breeding* **134**:384–393 DOI [10.1111/pbr.12289](https://doi.org/10.1111/pbr.12289).

- Wang M, Zou Z, Li Q, Sun K, Chen X, Li X. 2017.** The CsHSP17.2 molecular chaperone is essential for thermotolerance in *Camellia sinensis*. *Scientific Reports* **7**:1237 DOI [10.1038/s41598-017-01407-x](https://doi.org/10.1038/s41598-017-01407-x).
- Waters ER. 2013.** The evolution, function, structure, and expression of the plant sHSPs. *Journal of Experimental Botany* **64**:391–403 DOI [10.1093/jxb/ers355](https://doi.org/10.1093/jxb/ers355).
- Waters ER, Aebermann BD, Sanders-Reed Z. 2008.** Comparative analysis of the small heat shock proteins in three angiosperm genomes identifies new subfamilies and reveals diverse evolutionary patterns. *Cell Stress Chaperones* **13**:127–142 DOI [10.1007/s12192-008-0023-7](https://doi.org/10.1007/s12192-008-0023-7).
- Yang Z, Wang Y, Gao Y, Zhou Y, Zhang E, Hu Y, Yuan Y, Liang G, Xu C. 2014.** Adaptive evolution and divergent expression of heat stress transcription factors in grasses. *BMC Evolutionary Biology* **14**:147 DOI [10.1186/1471-2148-14-147](https://doi.org/10.1186/1471-2148-14-147).
- Zeng JK, Li X, Zhang J, Ge H, Yin XR, Chen KS. 2016.** Regulation of loquat fruit low temperature response and lignification involves interaction of heat shock factors and genes associated with lignin biosynthesis. *Plant Cell and Environment* **39**:1780–1789 DOI [10.1111/pce.12741](https://doi.org/10.1111/pce.12741).
- Zhang J, Liu B, Li J, Zhang L, Wang Y, Zheng H, Lu M, Chen J. 2015.** Hsf and Hsp gene families in *Populus*: genome-wide identification, organization and correlated expression during development and in stress responses. *BMC Genomics* **16**:181 DOI [10.1186/s12864-015-1398-3](https://doi.org/10.1186/s12864-015-1398-3).
- Zhang R, Pan B, Li Y, Li X. 2019.** SNP rs4937333 in the miRNA-5003-binding site of the ETS1 3'-UTR decreases ETS1 expression. *Frontiers in Genetics* **10**:581 DOI [10.3389/fgene.2019.00581](https://doi.org/10.3389/fgene.2019.00581).